Preprints of the 21st IFAC World Congress (Virtual)
Berlin, Germany, July 12-17, 2020

Empirical Battery Modelling for High Currents: The Effect of Nonlinear Overpotential and Inevitable Self-Heating

F.S.J. Hoekstra * **Y.J.J. Heuts** * **H.J. Bergveld** *,** **M.C.F. Donkers** *

* *Department of Electrical Engineering, Eindhoven University of Technology, Netherlands (e-mail: {f.s.j.hoekstra, h.j.bergveld, m.c.f.donkers}@tue.nl and y.j.j.heuts@student.tue.nl)*
** *NXP Semiconductors, Eindhoven, Netherlands*

Abstract: Electric race cars are a challenging application for battery management. The main issue is that the use of extremely high currents leads to additional nonlinear behaviour in the battery. The source of this nonlinear behaviour can be found in the nonlinear Butler-Volmer relation between currents and overpotentials, as well as self-heating that occurs when large currents are drawn due to the electrical resistance of the battery. As a result, nonlinearities in the input-output behaviour are caused by both factors. To accurately model the nonlinear overpotential behaviour using empirical battery models, it is necessary to be able to distinguish between the contribution of both sources of nonlinearities. In this paper, this problem is tackled by identifying a temperature- and current-dependent electrical model on lap data of an electric race car using a global approach to estimating state-space linear parameter-varying models. To aid the distinction between both effects, the influence of the temperature on the behaviour is distilled from local data, i.e., at constant temperatures. This is used as initialisation for the global optimisation problem, which identifies the effect of both phenomena from a single data set. Lap data of four race cycles is available. One cycle is used for parameter estimation of the battery model and the other three are used to validate the model. The results show that this approach brings a significant improvement to the modelling accuracy and presents opportunities to develop BMS applications, such as state estimators or even online power limiters for extreme battery-electric-vehicle applications.

Keywords: Battery management, Linear parameter-varying, Nonlinear systems, Electric and solar vehicles, Battery modelling.

1. INTRODUCTION

Electrification of vehicles is becoming increasingly more common. This practice is motivated by the need for energy independence and reduction of local and global pollution (Zhou et al., 2015). Initially, the electrification mainly focused on consumer-directed automotive applications, i.e., passenger cars, but it is now also expanding to maritime and aviation applications. As electric passenger cars are slowly becoming mainstream, electrification of cars also expands to racing applications, such as Formula E.

For an electric race car, it is important to be able to predict how many laps can be completed before a pit-stop for charging is required. Whether or not the car is able to complete a lap, is mainly determined by the electrical behaviour of the battery. This means that none of the cells in the pack should violate the lower voltage limit, otherwise the cells are exposed to dangerous operating conditions. If this happens, the battery management system will shut down the power flow of the battery pack and the car will come to a standstill. To prevent this scenario, it is vital that the electrical behaviour of the battery pack can be predicted in an accurate and computationally efficient manner.

Modelling the electrical behaviour of batteries is extensively covered in the literature. Roughly speaking, all models can be divided into two categories, namely physics-based models and data-driven models, see (Zhang et al., 2014). While the former are interesting for understanding the internal workings of a battery on a physical level, they are computationally expensive and do not necessarily produce the best Input-Output (IO) predictions, as shown in (Beelen, 2019). Alternatively, data-driven models such as Equivalent-Circuit Models (ECMs) or empirical models can be used, see (Fotouhi et al., 2016). These models require limited computational power and can accurately predict the IO behaviour of a battery, as shown in (Hu et al., 2012). At constant operating conditions, i.e., constant State-of-Charge (SoC) or temperature, the battery behaviour is locally linear and can thus be well-described by a linear ECM (with the exception of low SoC at which minor local nonlinearities are found as described in (Relan et al., 2017)). However, globally the behaviour is nonlinear and this can be captured accurately using Linear Parameter-Varying (LPV) models, see, e.g., (Hu

and Yurkovich, 2010), in which the parameters depend on the operating conditions.

In electric race cars, a particular challenge is to accurately model the effect of high currents, i.e., peak currents of up to 20C. In (Liu et al., 2015) and (Juang et al., 2013), it is found that such high currents can induce a nonlinear overpotential. The reason for this is argued to be the Butler-Volmer equation, which describes how the reaction current depends on the overpotential at the surface of the electrode, and is given by

$$i = i_0(e^{\frac{\alpha_1 F}{RT}\eta} - e^{\frac{\alpha_2 F}{RT}\eta}) \tag{1}$$

where i is the current density, i_0 the exchange current density, R is the universal gas constant, F is Faraday's constant, T is the absolute temperature, η is the overpotential and α_1 and α_2 are the electrode transfer coefficients for reduction and oxidation, respectively, as described in (Di Domenico et al., 2010). A common approximation is $\alpha_1 = \alpha_2 = 0.5$, which simplifies (1) and allows it to be rewritten as

$$\eta = \frac{RT}{F}\sinh^{-1}(\frac{i}{2i_0}) \tag{2}$$

where the inverse hyperbolic sine represents the nonlinearity in the overpotential. Although this phenomenon is captured in (Liu et al., 2015) and (Juang et al., 2013), the presence of significant self-heating, which occurs as a result of high current discharge, is not addressed. The influence of temperature on the cell behaviour is significant, see, e.g., (Ye et al., 2012). Therefore, it is difficult to sufficiently excite the cell's dynamics, such that a model can be identified, without altering its temperature. This requires an estimation approach that can deal with both the presence of varying temperature and nonlinearity induced by high currents.

In this paper, a temperature- and current-dependent electrical model is identified on lap data of an electric race car using a global State-Space (SS)-LPV approach, see (Cox, 2018). In order to distinguish between the effects of temperature and current, first an LPV model is identified which only depends on the temperature. This is done by exciting the cell using scaled-down race profiles at constant temperatures. The temperature dependency is captured in basis functions and these are supplied as initialisation for the global approach, which identifies both the effect of the current, by choosing between multiple nonlinear inputs, and the temperature. The global approach minimises the prediction error using a gradient-based Gauss-Newton algorithm of (Cox, 2018), which is based on (Wills and Ninness, 2008). The methods and obtained accuracies will be validated on different race data than the one that is used to identify the models. The proposed approach allows the simultaneous identification of a model that captures the nonlinear contribution of both the temperature and high currents to the overpotential. To the authors' knowledge, no such approach exists in the literature. A model that accurately describes the voltage during such dynamic scenarios can be used for applications as for instance SoC estimation or to predict power limits.

The remainder of this paper is structured as follows: Section 2 presents the available data of an electric race car and illustrates that a Linear Time-Invariant (LTI) model does not provide satisfactory predictions in this

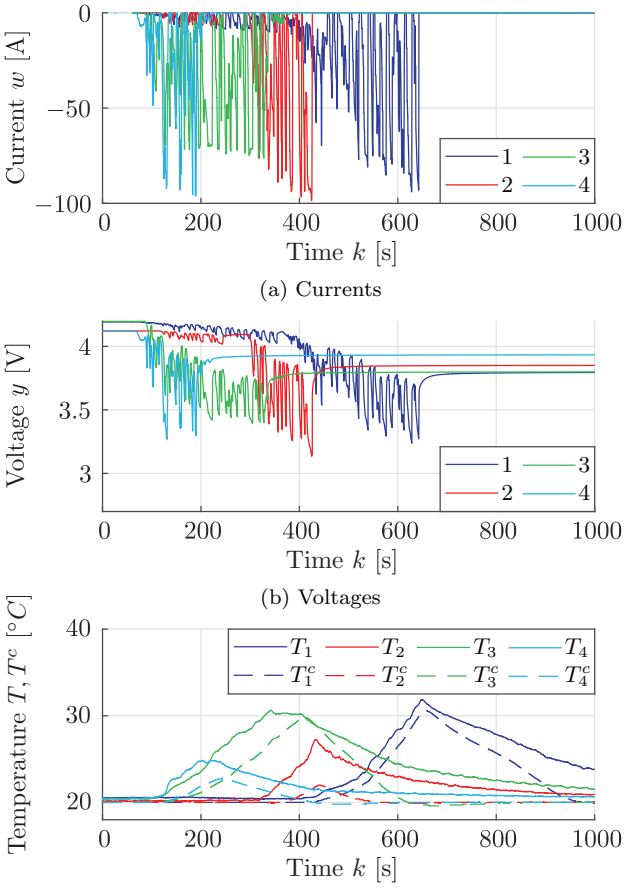

(a) Currents

(b) Voltages

(c) Surface temperature (T) and chamber temperature (T^c)

Fig. 1. Four race cycles (1, 2, 3, 4) repeated on test setup.

situation. A modelling approach that can identify and distinguish between the nonlinearities associated with the temperature and current is presented in Section 3. The modelling and validation results are presented in Section 4 and, finally, conclusions are drawn in Section 5.

2. AVAILABLE DATA AND MOTIVATING EXAMPLE

Available to us is a data set of an electric race car, containing the pack current, pack voltage and cooling fluid temperature measured during 4 different races. The experiments are reproduced on a single cell in a dedicated battery test setup, consisting of a computer controlled thermal chamber, and electrical load and supply, to obtain reliable measurements and to be able to measure the surface temperature of the cell. The cell under consideration is a Kokam SLPB11543140H5 high-power lithium-nickel-manganese-cobalt-oxide cell, with a nominal capacity of 5 Ah. This cell can sustain continuous discharge currents of up to 30C and peak currents of 50C. Profile 1 and 2 are prepended with a scaled-down version of their profiles, to also capture the dynamics at low currents. The current profiles, resulting terminal voltages, surface temperatures and ambient chamber temperatures (set to be the temperature of the cooling fluid) are shown in Fig. 1.

In order to demonstrate the significant nonlinearity that is present in the overpotential, an LTI overpotential model has been fitted in a Least-Squares (LS) fashion on the scaled-down part of Profile 1. This allows the model to

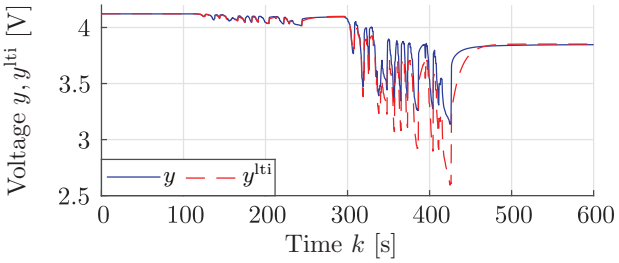

Fig. 2. Comparison of simulated (y^{lti}) and measured voltage using Profile 2.

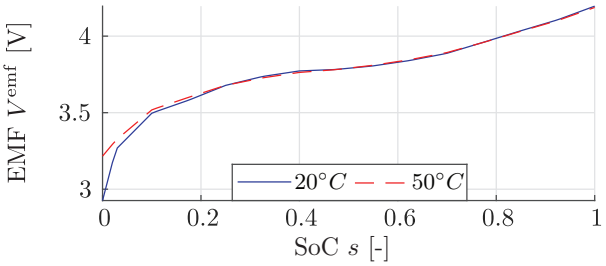

Fig. 3. Temperature-dependent EMF.

capture the same dynamics that are present in the race cycles, the importance of which is explained in (Beelen et al., 2018). However, by only considering low currents, the effect of self-heating is avoided. The model has then been used to simulate Profile 2 and this has been compared to the measured voltage, as shown in Fig. 2. As the cycle progresses, and the current and thus the temperature increases, the simulated voltage strays far from the measured voltage. This discrepancy motivates the need for a model that can capture these nonlinearities.

3. BATTERY MODELLING

The behaviour of the battery can be modelled using a discrete-time nonlinear model. The state evolution and output of the model are given by

$$\begin{cases} \begin{bmatrix} s_{k+1} \\ o_{k+1} \end{bmatrix} = \begin{bmatrix} 1 & 0 \\ 0 & A(T_k) \end{bmatrix} \begin{bmatrix} s_k \\ o_k \end{bmatrix} + \begin{bmatrix} \frac{\delta}{C_0} \\ B(T_k) \end{bmatrix} w_k, \\ y_k = V^{\text{emf}}(s_k, T_k) + Co_k + D(T_k)w_k, \end{cases} \tag{3}$$

where $o_k \in \mathbb{R}^{m_0}$ is the dynamic part of the overpotential, with m_0 the number of overpotential states ($m_o = 1$ in this paper), s_k is the SoC, which satisfies $0 \leq s_k \leq 1$ for all time $k \in \mathcal{K} = \{0, \ldots, K\}$, with K the maximum time instant. Furthermore, y_k is the terminal voltage, w_k is the input current, $\delta = 0.01$s is the sampling time, T_k is the (surface) temperature of the cell and V^{emf} is a nonlinear function of s and T describing the Electromotive-Force (EMF) of the cell, which is often referred to as the open-circuit voltage. The matrices $A(T) \in \mathbb{R}^{m_0 \times m_0}$, $B(T) \in \mathbb{R}^{m_0 \times 1}$ and $D(T) \in \mathbb{R}^{1 \times 1}$ are temperature dependent. The SS model is written in observable canonical form, i.e., $C = \mathbf{1} \in \mathbb{R}^{1 \times m_o}$, such that captured dynamics are consistently attributed to the same parameters.

Parameterising (3) is commonly done by separating the problem into two parts, namely determining the underlying nonlinear EMF V^{emf} and capacity C_0, and secondly identifying the locally linear overpotential model, i.e., the dynamic part of the terminal voltage as a result of excitation, captured by A, B and D. Both V^{emf} and the SS matrices can be modelled as a function of SoC, temperature and current. However, in this paper only discharging is considered, which allows us to discard the dependence on the current direction in the form of hysteresis in the EMF and asymmetric overpotential. Moreover, the dependency of the overpotential model on the SoC is also neglected since this dependency is not significant in the SoC range 1 to 0.2, see (Jiani et al., 2014). Below that SoC, it is not possible to draw currents of the magnitude presented in Fig. 1a, without violating the lower voltage limit. Therefore, these dynamics are also not represented in the data sets and the dynamics are only dependent on the temperature. In this section, the procedure for mapping the EMF is discussed first, followed by a description of the approach for modelling the overpotential.

3.1 Electromotive-Force Modelling

There are multiple approaches to mapping the EMF as a function of SoC and temperature. A popular approach is to do a slow charge and discharge, i.e., using small current rates of C/30 or C/40, as described in (Pattipati et al., 2014). The EMF lies in-between the curves, but where exactly is uncertain, due to the asymmetric nature of the overpotential and the possible presence of hysteresis. Moreover, these long experiments are prone to current sensor bias, resulting in an unreliable mapping with respect to the SoC. Alternatively, one can use extrapolation to zero current, as proposed in (Shadman Rad et al., 2013). Although this method tackles the problem of asymmetry, it still copes with the problem of sensor bias. Therefore, the third option is the approach of pulsed current experiments in which the cell is discharged with pulses and subsequently rested such that the overpotential relaxes to zero and the terminal voltage equals the EMF, see, e.g., (Pop et al., 2006). The use of pulses allows the use of higher currents, leading to a smaller signal-to-noise ratio for the current measurement and it also enables the detection and correction of sensor bias. The pulse-discharge method is compared to the first method and is deemed to be the most accurate in (Petzl and Danzer, 2013) and (Pop et al., 2006). The only drawback of this method is the significant experiment time, which comes with the risk of self-discharge.

In this paper, only discharging is considered. Therefore, the EMF is obtained using a pulse-*discharge* experiment. Each pulse extracts approximately 7.5% SoC and the EMF at in-between SoC values is determined using linear interpolation. The experiment has been performed at 20 and $50°C$ to model the temperature dependence. The capacity C_0 is defined as the discharged capacity at $20°C$. By choosing a fixed capacity C_0, instead of one that depends on the temperature, the oddity of a temperature-dependent SoC is avoided. The EMF curves for the two temperatures are shown with respect to the SoC in Fig. 3.

3.2 Overpotential Modelling

When modelling the overpotential, it is important to accurately capture the effect of both the temperature and

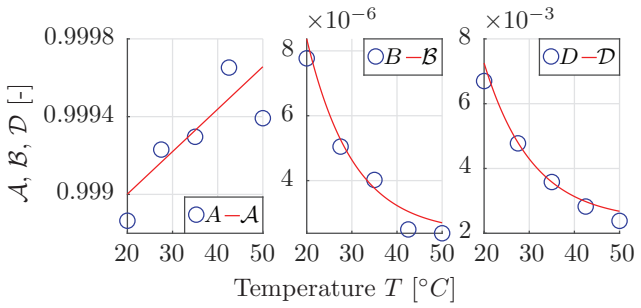

Fig. 4. Local estimates (blue circles), combined with functional approximations (red line).

the high current. Differentiating between the two can be done by separating their effects. Since the problem of high currents is that they induce self-heating, the only possible separation is to first identify the temperature dependence locally.

Temperature Dependence To identify the dependence of the cell behaviour on temperature, the cell is excited at $\mathcal{T} = \{20, 27.5, 35, 42.5, 50\}^\circ C$ using a scaled-down version of Profile 1, with a maximum discharging current of 2C, thus preventing self-heating. First, the overpotential is determined by subtracting the EMF from the terminal voltage

$$y^o = y - V^{\text{emf}}(s, T) \tag{4}$$

where y^o is the overpotential. A first-order Auto-Regressive model with eXogenous inputs (ARX) has been selected to model the dynamics, since the behaviour is primarily of first order, see (Hu and Yurkovich, 2011). Therefore, the overpotential is given by the difference equation

$$\hat{y}^o_k = -a_1 y^o_{k-1} + b_0 w_k + b_1 w_{k-1} \tag{5}$$

where a_1, b_0 and b_1 are the model parameters estimated by solving the LS minimisation problem

$$\min_{a_1, b_0, b_1} \quad \sum_{k=1}^{K} \|y^o_k - \hat{y}^o_k\|_2^2 \text{ for all } k \in \mathcal{K}. \tag{6}$$

Subsequently, (5) can be written in SS format as

$$o_{k+1} = -a_1 o_k + (b_1 - a_1 b_0) w_k \tag{7a}$$
$$\hat{y}^o_k = o_k + b_0 w_k. \tag{7b}$$

By repeating this process for all $T \in \mathcal{T}$, a temperature-dependent LPV model has been constructed, where matrices $A(T)$, $B(T)$ and $D(T)$ are spline-interpolated lookup tables, the data points of which are represented by the blue circles in Fig. 4. After adding V^{emf} to its output, the results of the model are referred to as y^{Tlpv}, which stands for *Temperature*-dependent *linear parameter-varying* modelled battery voltage.

High Current and Temperature Dependence Having established the influence of the temperature on the model parameters, we will proceed to identify the influence of the current on the overpotential behaviour. In (Juang et al., 2013), it is noted that the current rate only influences the diffusion behaviour, i.e., the behaviour captured by (9a). The nonlinear influence of the current is captured by transforming the input of (9a) to $\sinh^{-1}(\alpha w_k)$, derived from (2), where α is a to-be-established scaling factor. To capture the effect of the nonlinearity induced by the current and to simultaneously deal with the dynamic temperature encountered in racing profiles, a global LPV SS identification procedure is applied. The term global indicates that the scheduling variable, in this case temperature, varies in the data. This opposed to the local approach, used to obtain the temperature-dependent LPV model, where multiple LTI models are fitted on data in which the scheduling variable is fixed, i.e., the temperature is constant. For a more detailed explanation, see (Tóth, 2010). The global procedure applied here minimises the prediction error using a gradient-based algorithm, which uses a Gauss-Newton scheme, as described in (Cox, 2018).

This approach requires the temperature dependence to be described by a specific basis function. Fig. 4 shows that the dependency of B and D can be captured well using an exponential function. The dependency of A on the temperature has a higher variance, but is nevertheless best described using an affine basis function, which results in

$$\mathcal{A}(T) = c_a + d_a T, \mathcal{B}(T) = c_b + d_b e^{\beta_b T}, \mathcal{D}(T) = c_d + d_d e^{\beta_d T}, \tag{8}$$

where the calligraphic $\mathcal{A}$, $\mathcal{B}$ and $\mathcal{D}$ are the functional versions of the SS parameters A, B and D, and they are parametrised through c_a, d_a, c_b, d_b, β_b, c_d, d_d and β_d which are fitted in an LS fashion on the local estimates (represented by the blue circles in Fig. 4), the result of which is shown by red lines in Fig. 4.

The parameter α does not appear in (8), but can be incorporated by formulating the model as follows

$$o_{k+1} = \mathcal{A}(T) o_k + \begin{bmatrix} \mathcal{B}^0(T) \\ \mathcal{B}^1(T) \\ \vdots \\ \mathcal{B}^n(T) \\ \vdots \\ \mathcal{B}^N(T) \end{bmatrix}^\top \begin{bmatrix} w_k \\ \sinh^{-1}(\alpha_1 w_k) \\ \vdots \\ \sinh^{-1}(\alpha_n w_k) \\ \vdots \\ \sinh^{-1}(\alpha_N w_k) \end{bmatrix} \tag{9a}$$

$$\hat{y}^o_k = o_k + \mathcal{D}(T) w_k, \tag{9b}$$

where α is now split into α_1 to α_N, with $n \in \mathcal{N} = \{1, \ldots, N\}$ and N the number of segmentations of α. The nonlinear optimisation problem is now given by

$$\min_{\mathcal{A}, \mathcal{B}^0, \mathcal{B}^n, \mathcal{D}} \quad \frac{1}{K} \sum_{k=1}^{K} \|y^o_k - \hat{y}^o_k\|_2^2 \text{ for all } k \in \mathcal{K}, \tag{10}$$

with $n \in \mathcal{N}$ and where the prediction-error minimisation scheme only adapts the affine parameters, i.e., c and d in (8). The correct amount of nonlinearity in the input is thus determined by the algorithm by adjusting the parameters in $\mathcal{B}^0$ and $\mathcal{B}^n$. As a result, there is no need to exactly determine α. The model of this form is a *temperature*-dependent *nonlinear parameter-varying* model and its results, added to V^{emf}, will be referred to as y^{Tnlpv}.

4. MODELLING RESULTS AND VALIDATION

In this section, the proposed model structure ($Tnlpv$) is parameterised using the race data of Profile 1 and two local temperature data sets. The model is validated on the additional three race profiles and the performance is compared to the LTI model and the temperature-dependent model ($Tlpv$).

4.1 Model Parametrisation

Using the form of (9), we still need to establish what value for N is appropriate, what values for α_n should be used, and how all the parameters should be initialised. Regarding the value of N, it has been found that $N = 2$ is the best choice. Any $N > 2$ results in numerical instability of the optimisation problem. Selecting $N = 1$ results in slightly worse to similar modelling precision, as will be shown in the results. However, choosing $N = 1$ requires an extensive search for the correct value of α. Instead, by choosing $N = 2$ we can select α_1 and α_2 as boundaries of our searching range and the algorithm will weigh their individual contribution such that their addition, through (9a), captures the complete nonlinearity. A rough grid search has been applied to find two values in-between which the true α most likely lies. This suggests that α should lie in-between 0.15 and 0.2, thus $\alpha_1 = 0.15$ and $\alpha_2 = 0.2$ have been used for the cell under consideration. For correct initialisation, which is important because this is a nonlinear optimisation problem, $\mathcal{A}$ and $\mathcal{D}$ are initialised as the values fitted on the local estimates, as shown in Fig. 4. Since the behaviour of the overpotential state should be mainly ruled by the augmented inputs, $\mathcal{B}^n$ have also been initialised as the local models and the parameters of $\mathcal{B}^0$ have been initialised as zero. A case for $N = 1$ is also included for comparison, in this case $\alpha = 0.175$.

Profile 1, combined with two local data sets at 27.5 and 35°C, is used as y^o in (10) to determine the parameters. The inclusion of the two local data sets is necessary, as otherwise not all behaviour is represented in the data set. As a result, certain behaviour would then be attributed to temperature, while in fact it is caused by high currents. A comparison of the performance of the LTI model, the temperature-dependent LPV model and the temperature-dependent and current-influenced NLPV model is made and results are shown in Fig. 5 and the Root-Mean-Square (RMS) errors are reported in Table 1. The results clearly show the improvement of considering both temperature and the nonlinear effect of large currents when modelling the cell behaviour for racing conditions. Fig. 5b shows that the nonlinearity of the current is indeed only associated with the state behaviour, since only considering the temperature already produces the correct instant voltage drops, modelled by the direct-feedthrough term $\mathcal{D}$.

Table 1. RMS errors Profile 1 in mV

Profile	y^{lti}	y^{Tlpv}	$y^{\text{Tnlpv}}_{N=1}$	$y^{\text{Tnlpv}}_{N=2}$
1	126	58.1	8.00	7.80

4.2 Model Validation

In order to validate the model performance, the three models have been used once more to simulate the voltage of Profiles 2 to 4. The results are presented in Fig. 6 and the RMS errors are listed in Table 2. These results demonstrate the effectiveness and necessity for taking into account the nonlinearity of the current *and* temperature. Moreover, the importance of considering the correct temperature measurement, i.e., on the surface instead of the chamber temperature, is demonstrated in Fig. 7 and the RMS errors are shown in Table 3. In this case, both models show a distinct mismatch with the measurement. It should be noted that although using the surface temperature does provide more accurate predictions, the performance could be even better if the internal temperature were to be used. This is especially true in the case of self-heating, where heat is generated from within. In this study, the cell was relatively small, so the difference between the internal and the surface temperature is also assumed to be small. However, this should definitely be a point of concern for larger cells.

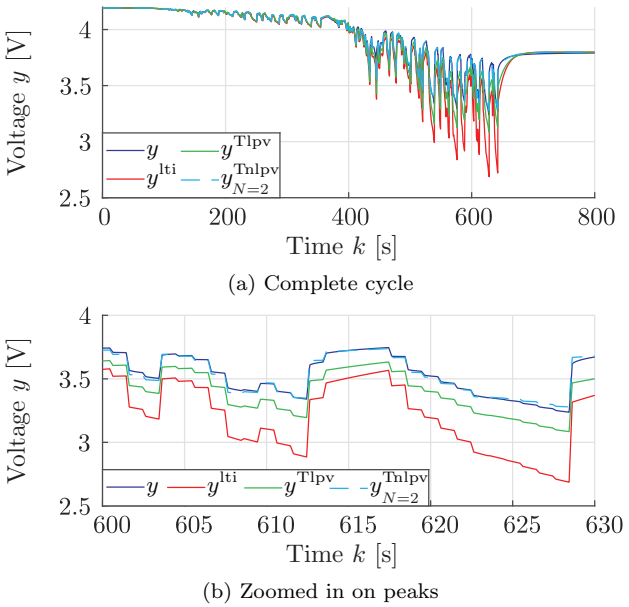

(a) Complete cycle

(b) Zoomed in on peaks

Fig. 5. Model performance on Profile 1.

Table 2. RMS errors Profile 2 to 4 in mV

Profile	y^{lti}	y^{Tlpv}	$y^{\text{Tnlpv}}_{N=1}$	$y^{\text{Tnlpv}}_{N=2}$
2	113	66.5	9.6	9.7
3	174	86.2	12.3	11.8
4	96.9	59.7	12.7	12.6

Table 3. RMS errors when considering T^c instead of T, listed in mV.

Profile	y^{Tlpv}	$y^{\text{Tnlpv}}_{N=2}$
3	118	45.1

5. CONCLUSION

In this paper, the importance of considering the nonlinearities associated with both the temperature and current in empirical battery modelling for high currents has been demonstrated. Moreover, a tool has been provided for modelling their combined effect on a dynamic data set, i.e., with varying temperature and current. The results show the accuracy of the proposed model and this work can naturally be extended to applications such as a power limiter. In order to make predictions on the electrical behaviour with this model, it is important to also have an accurate thermal model, so it is known how the temperature of the battery-cell or -pack will develop. This work can be further improved by determining whether or not the nonlinearity of the current is State-of-Charge- and temperature-dependent, as suggested in (Juang et al., 2013) and (Juang et al., 2014), respectively. Finally, applying this approach to large cells can lead to inaccuracy due to the difference between the surface and internal temperature.

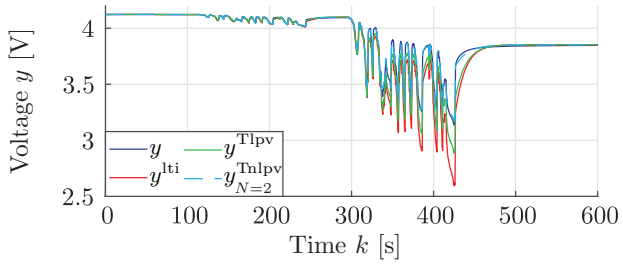

(a) Profile 2

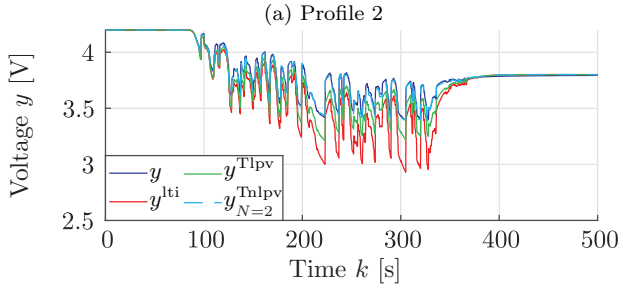

(b) Profile 3

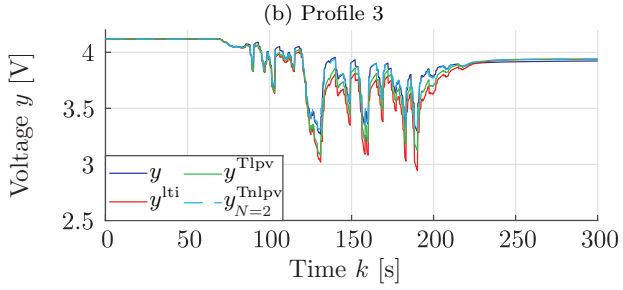

(c) Profile 4

Fig. 6. Model performance on Profiles 2 to 4.

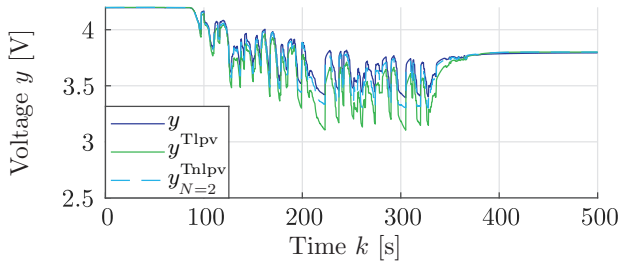

Fig. 7. Voltage results when considering T^c instead of T.

REFERENCES

Beelen, H. (2019). *Model-Based Temperature and State-of-Charge Estimation for Li-ion Batteries*. Ph.D. thesis, Eindhoven University of Technology.

Beelen, H., Bergveld, H., and Donkers, M. (2018). On Experiment Design for Parameter Estimation of Equivalent-Circuit Battery Models. In *IEEE Conf. on Control Tech. and Applications*, Copenhagen.

Cox, P. (2018). *Towards Efficient Identification of Linear Parameter-Varying State-Space Models*. Ph.D. thesis, Eindhoven University of Technology.

Di Domenico, D., Stefanopoulou, A., and Fiengo, G. (2010). Lithium-Ion Battery State of Charge and Critical Surface Charge Estimation Using an Electrochemical Model-Based Extended Kalman Filter. *J. of Dyn. Systems, Meas., and Control*.

Fotouhi, A., Auger, D.J., Propp, K., Longo, S., and Wild, M. (2016). A review on electric vehicle battery modelling: From Lithium-ion toward Lithium–Sulphur. *Renew. and Sust. Energy Reviews*.

Hu, X., Li, S., and Peng, H. (2012). A comparative study of equivalent circuit models for Li-ion batteries. *J. Power Sources*.

Hu, Y. and Yurkovich, S. (2010). Battery state of charge estimation in automotive applications using LPV techniques. In *Proc. American Control Conf.*

Hu, Y. and Yurkovich, S. (2011). Linear parameter varying battery model identification using subspace methods. *J. Power Sources*.

Jiani, D., Zhitao, L., Youyi, W., and Changyun, W. (2014). A fuzzy logic-based model for Li-ion battery with SOC and temperature effect. In *IEEE Int. Conf. on Control & Automation*.

Juang, L.W., Kollmeyer, P.J., Jahns, T.M., and Lorenz, R.D. (2014). Improved modeling of lithium-based batteries using temperature-dependent resistance and overpotential. In *IEEE Transportation Electrification Conf. and Expo*.

Juang, L.W., Kollmeyer, P.J., Jahns, T.M., and Lorenz, R.D. (2013). Improved Nonlinear Model for Electrode Voltage–Current Relationship for More Consistent Online Battery System Identification. *IEEE Trans. Ind Appl*.

Liu, S., Jiang, J., Shi, W., Ma, Z., Wang, L.Y., and Guo, H. (2015). Butler–Volmer-Equation-Based Electrical Model for High-Power Lithium Titanate Batteries Used in Electric Vehicles. *IEEE Trans. Ind. Electron*.

Pattipati, B., Balasingam, B., Avvari, G., Pattipati, K., and Bar-Shalom, Y. (2014). Open circuit voltage characterization of lithium-ion batteries. *J. Power Sources*.

Petzl, M. and Danzer, M.A. (2013). Advancements in OCV Measurement and Analysis for Lithium-Ion Batteries. *IEEE Trans. Energy Convers*.

Pop, V., Bergveld, H.J., Op het Veld, J.H.G., Regtien, P.P.L., Danilov, D., and Notten, P.H.L. (2006). Modeling Battery Behavior for Accurate State-of-Charge Indication. *J. Electrochemical Society*.

Relan, R., Firouz, Y., Timmermans, J.M., and Schoukens, J. (2017). Data-Driven Nonlinear Identification of Li-Ion Battery Based on a Frequency Domain Nonparametric Analysis. *IEEE Trans. Control Syst. Technol*.

Shadman Rad, M., Danilov, D., Baghalha, M., Kazemeini, M., and Notten, P. (2013). Adaptive thermal modeling of Li-ion batteries. *Electrochim. Acta*.

Tóth, R. (2010). *Modeling and Identification of Linear Parameter-Varying Systems*, volume 403 of *Lecture Notes in Control and Information Sciences*. Springer Berlin Heidelberg, Berlin, Heidelberg.

Wills, A. and Ninness, B. (2008). On Gradient-Based Search for Multivariable System Estimates. *IEEE Trans. on Automatic Control*.

Ye, Y., Shi, Y., Cai, N., Lee, J., and He, X. (2012). Electro-thermal modeling and experimental validation for lithium ion battery. *J. Power Sources*.

Zhang, C., Li, K., Mcloone, S., and Yang, Z. (2014). Battery modelling methods for electric vehicles - A review. In *Proc. European Control Conf.*

Zhou, Y., Wang, M., Hao, H., Johnson, L., Wang, H., and Hao, H. (2015). Plug-in electric vehicle market penetration and incentives: a global review. *Mitig Adapt Strateg Glob Change*.